Deformable Registration of Diffusion Tensor MR Images with Explicit Orientation Optimization

Hui Zhang[1], Paul A. Yushkevich[2], and James C. Gee[2]

[1] Department of Computer & Information Science, University of Pennsylvania, USA
[2] Department of Radiology, University of Pennsylvania, USA

Abstract. In this paper we present a novel deformable registration algorithm for diffusion tensor (DT) MR images that enables explicit analytic optimization of tensor reorientation. The optimization seeks a piecewise affine transformation that divides the image domain into uniform regions and transforms each of them affinely. The objective function captures both the image similarity and the smoothness of the transformation across region boundaries. The image similarity enables explicit orientation optimization by incorporating tensor reorientation, which is necessary for warping DT images. The objective function is formulated in a way that allows explicit implementation of analytic derivatives to drive fast and accurate optimization using the conjugate gradient method. The optimal transformation is hierarchically refined in a subdivision framework. A comparison with affine registration for inter-subject normalization of 8 subjects shows that our algorithm improves the alignment of manually segmented white matter structures (corpus callosum and cortio-spinal tracts).

1 Introduction

Diffusion tensor magnetic resonance imaging (DT-MRI)[1] is a water diffusion imaging technique that has been used to provide unique insight into the white matter (WM) organization in human brains [2, 3]. Diffusion describes the random movement of molecules. The rate of diffusion at a point, as a function of spatial direction, is refered to as a *diffusion profile*. This function can be sampled by acquiring a series of MR images sensitized to diffusion in a set of selected directions. In DT-MRI, diffusion profiles are assumed to be Gaussian and are defined by 2nd-order symmetric tensors. A DT image is produced by fitting this model to sampled diffusion profiles in each voxel of the MR series. The way in which DT describes local water diffusion can be best understood through its eigenvectors and eigenvalues. The eigenvectors of a DT coincide with the three principal directions of diffusion while the corresponding eigenvalues measure the rates of diffusion in those directions. In fibrous tissue, such as WM, although water is free to diffuse along the axis of the axon fiber bundles, diffusion is hindered in perpendicular directions by myelin that bound the axons. Consequently, the principal eigenvectors of the DTs measured in these regions tend to be parallel to the axis of the axon bundles. Compared to conventional MR images, this

J. Duncan and G. Gerig (Eds.): MICCAI 2005, LNCS 3749, pp. 172–179, 2005.

unique ability of DT images to reveal the orientation of axon bundles makes the modality an ideal choice for understanding and analyzing WM structures.

The ability to detect WM differences between pairs and groups of subjects is essential in studying the pathology of various neurological disorders that are associated with WM abnormalities and may prove useful in early detection. To enable such group comparison analysis using DT images, a registration method is required [4, 5]. Compared to registering scalar images, the registration of DT images is particularly challenging not only due to the multi-dimensionality of the data, but also because one must ensure that the DT orientations remain consistent with the anatomy after image transformations [6]. Current DT registration techniques either circumvent tensor reorientation by registering scalar images derived from DT images, thus discarding the orientation component of the data, or perform tensor reorientation iteratively rather than analytically, thus precluding direct applications of gradient methods (see [7] for a survey).

In this paper we describe a novel algorithm for deformable registration of DT images that incorporates explicit optimization of tensor reorientation in an analytic manner. The optimization seeks a piecewise affine transformation that divides the image domain into uniform regions, each of which is transformed affinely. The objective function optimizes both the image similarity and the smoothness of the transformation across contiguous regions. The piecewise nature of the candidate transformations allows us to express the image similarity as the sum of the region similarities. Individual region similarity is computed using our previously published affine registration algorithm [8] which incorporates tensor reorientation in its objective function analytically, allowing explicit orientation optimization. The smoothness criterion imposed on the transformation is adapted from classic optical flow estimation [9], and it takes an analytic form as well. The resulting algorithm is based on analytic derivatives and uses the conjugate gradient method for optimization. By applying our algorithm to inter-subject registration, we demonstrate the algorithm is computationally efficient and improves the quality of image alignment.

In section 2, we will first briefly review the properties of DT images and the affine registration algorithm, then present our new piecewise affine formulation, and finally discuss the details of registration evaluation. The results of applying our algorithm to eight different subjects and their evaluations are shown and discussed in section 3.

2 Method

A diffusion tensor $\mathbf{D}$ is a symmetric and positive-definite (SPD) 2nd-order tensor, which is related to a Gaussian diffusion profile $d_{\mathbf{D}}(\hat{k})$ by the quadratic form

$$d_{\mathbf{D}}(\hat{k}) = \hat{k}^{\mathrm{T}}\mathbf{D}\hat{k}, \tag{1}$$

where $\hat{k}$ is a unit vector defined over the unit sphere $\mathbb{S}^2$. By measuring values of $d_{\mathbf{D}}(\hat{k})$ for different $\hat{k}$, $\mathbf{D}$ can be determined through (1) by least square fitting.

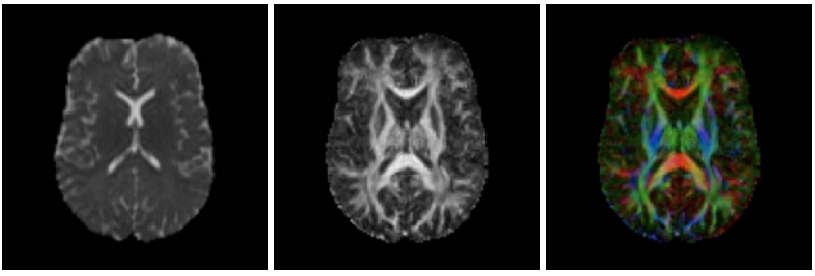

Fig. 1. The axial slice 24 of the DT image chosen as the template in this study. From left to right are the trace, the FA and the color-coded principal eigenvector maps. The latter is scaled by the FA map and the directions encoded by each color channel are mediolateral for red, anteroposterior for green and superoinferior for blue.

Because $\mathbf{D}$ has six independent components, measurements from a minimum of 6 independent directions have to be acquired.

Two useful transformation-invariant scalar indices for $\mathbf{D}$ are its trace and fractional anisotropy (FA). The trace is proportional to the mean diffusivity. Because the cerebrospinal fluid (CSF) has the most freely diffusing water, it appears the brightest in trace maps. The FA values vary from 0 for isotropic diffusion, such as in CSF and grey matter (GM), to 1 for anisotropic diffusion, such as in WM. Thus the WM is highlighted in FA maps. To illustrate WM fiber bundle orientation, a popular method is to use the principal eigenvector map [10] scaled by FA in which the orientation is encoded in terms of color. The stark difference between FA and principal eigenvector maps is the best illustration of the rich orientation information contained in DT images. An example of these maps is shown in fig. 1.

When measuring the similarity of two DTs, various metrics are available. Given no clear consensus on what the best metric may be, we have chosen to compare three different metrics that are defined using the following inner products:

$$< \mathbf{D}_1, \mathbf{D}_2 >= \begin{cases} Tr(\mathbf{D}_1)Tr(\mathbf{D}_2) & (\text{for } \textit{trace distance}) \\ Tr(\mathbf{D}_1\mathbf{D}_2) & (\text{for } \textit{Euclidean distance}) \\ 2Tr(\mathbf{D}_1\mathbf{D}_2) + Tr(\mathbf{D}_1)Tr(\mathbf{D}_2) & (\text{for } L^2 \textit{ distance}) \end{cases},$$

with the actual distance given by $\|\mathbf{D}_1 - \mathbf{D}_2\| = \sqrt{< \mathbf{D}_1 - \mathbf{D}_2, \mathbf{D}_1 - \mathbf{D}_2 >}$. The trace distance (TD) between two tensors is the absolute value of the difference of their traces and is proportional to the difference of their mean rates of diffusion. The Euclidean distance (ED) is the Frobenius norm of the difference of two tensors. The ED reflects the relative orientation of the tensors and it is shown to perform better than the TD for DT registration [7]. The L^2 distance (LD) is defined in the functional space of diffusion profiles which is, generically, an infinite dimensional Hilbert space [8]. When applied to DTs, the LD is a weighted sum of the ED and the TD and our prior work suggests that it affords more robust registration over small regions [8] than each of those metrics does on its own.

2.1 Affine Registration Algorithm

The unique feature of our affine registration algorithm [8] is that the tensor reorientation is incorporated into the analytic objective function for explicit orientation optimization. This is accomplished by the combination of a special way of parameterizing the affine transform and a particular tensor reorientation strategy, which are described below.

An affine transformation F is parameterized as

$$F(x) = Mx + T = (QS)x + T, \tag{2}$$

where M, the Jacobian matrix of F, is parameterized based on its polar decomposition in terms of Q, an orthogonal matrix with determinant 1 representing pure rotation, and S, a SPD matrix representing pure deformation. The matrix Q can be represented using the 3 Euler angles, the matrix S has 6 independent components and the translation T has 3 components. We use these 12 variables to parametrize the affine transformation F, and denote them by vector $\mathbf{p}$.

For tensor reorientation, we use the finite strain (FS) reorientation strategy [6]. We choose FS over the more accurate method, the preservation of principal directions (PPD), because the PPD method is not analytic but algorithmic, computationally expensive, and the difference in accuracy between the two methods is minor [7]. When an orthogonal transformation Q is applied to a tensor $\mathbf{D}$, the corresponding reorientation is given by $Q\mathbf{D}Q^{\mathsf{T}}$ [6]. For a non-orthogonal transformation M, the FS strategy finds the best orthogonal approximation, Q_M, to M and uses it for reorientation. Our method leverages the fact that the pure rotation component of the polar decomposition of M is precisely the best orthogonal approximation of M. Thus, in the framework of our method, FS reorientation can be formulated analytically, rather than using eigen-decomposition, as done in other methods.

The objective function of registration is then

$$O(\mathbf{p}) = \int_{\mathbb{R}^3} \|\mathbf{D}_s((QS)x + T) - Q\mathbf{D}_t(x)Q^{\mathsf{T}}\|^2 \, dx \ , \tag{3}$$

where $\mathbf{D}_t$ and $\mathbf{D}_s$ are the template (fixed) and subject (moving) DT images respectively. The derivatives of $O(\mathbf{p})$ can be computed analytically; for example, the derivative with respect to t_i, the i-th component of the translation T is

$$\frac{\partial O}{\partial t_i} = \int_{\mathbb{R}^3} 2 < \frac{\partial \mathbf{D}_s}{\partial x_i}, \mathbf{D}_s((QS)x + T) - Q\mathbf{D}_t(x)Q^{\mathsf{T}} > dx.$$

2.2 Piecewise Affine Algorithm

The piecewise algorithm we propose involves using our affine algorithm for region-wise matching, enforcing the overall smoothness of the warp via smoothness constraints on interfaces of regions.

We subdivide the template $\mathbf{D}_t$ into equal size regions denoted Ω_i. In general, each region, Ω_i, has 6 neighboring regions and thus 6 different interfaces. For

each region Ω_i in the template, the goal of the piecewise algorithm is to find an affine transformation F_i that gives the best match with the subject, under certain smoothness constraints that are described below.

We will refer to the collection of F_i over all possible regions as a piecewise affine transformation, denoted as $\mathbb{F}$. Because the transformation within each region is affine, the smoothness within a region is guaranteed. The smoothness of the piecewise affine transformation thus needs to be imposed only on region interfaces. Following the standard approach in optical flow estimation [9], we minimize the transformation discontinuities across interfaces, which is formulated for neighboring regions Ω_i and Ω_j as

$$\int_{\Omega_i \cap \Omega_j} \|F_i(x) - F_j(x)\| dx. \tag{4}$$

Similar to (3), analytic derivatives can be derived for (4).

If the number of regions in each dimension is n, the parameter space of this optimization problem has a dimension of $12n^3$. We subdivide the template hierarchically with n being 4, 8 and 16. At the finest subdivision level, the dimension of the parameter space is 49152. The ability to compute derivatives of (4) analytically allows us to take advantage of the conjugate gradient method, which is generally more efficient than optimization techniques that do not use derivatives, such as the Powell's direction set.

By construction, discontinuities across interfaces in the piecewise affine transformation can be minimized but not eliminated. Therefore, after the piecewise affine approximation to the underlying trasformation is estimated at the finest level, it is interpolated using the standard approach [11] to generate a smooth warp field which is then used to deform the subject into the space of the template with the PPD reorientation strategy discussed in section 2.1.

2.3 Registration Evaluation

Here we outline two voxel-based measures that are specific to DT images to quantify the quality of image alignment. They are used to evaluate our inter-subject registration results.

To evaluate the overall quality of matching, we compute the average overlap of eigenvalue-eigenvector pairs (AOE) [12] of all the WM voxels (FA ≥ 0.3) in the template and the corresponding voxels in the image to compare. The AOE measures, on average, the extent to which two tensors at each voxel are aligned; it is defined as

$$\frac{1}{N} \sum_{i=1}^{N} \frac{\sum_{j=1}^{3} \lambda_j^i \lambda_j'^i (\epsilon_j^i \cdot \epsilon_j'^i)^2}{\sum_{j=1}^{3} \lambda_j^i \lambda_j'^i}, \tag{5}$$

where λ_j^i, ϵ_j^i and $\lambda_j'^i$, $\epsilon_j'^i$ are the j-th eigenvalue-eigenvector pair at the i-th voxel location in the pair of images, and N is the total number of voxel locations to compare.

To assess the quality of local matching, we compute the average angular separation of the principal eigenvector (AAS) [6] in a region-specific manner as

in [13]. The AAS measures specifically how well the principal eigenvectors are aligned; it is defined as

$$\frac{\sum_{i=1}^{N} \sqrt{\mu_i \mu_i'} \arccos |\epsilon_1^i \cdot \epsilon_1'^i|}{\sum_{i=1}^{N} \sqrt{\mu_i \mu_i'}}, \tag{6}$$

where μ_i, ϵ_1^i and μ_i', $\epsilon_1'^i$ are the FA and the principal eigenvector at the i-th voxel location in both images. The two regions we have chosen are the corpus callosum (CC) and the cortico-spinal tracts (CST), which are manually segmented from the template.

3 Results

Here we report the results of inter-subject registration of eight subjects to the template shown in fig. 1. The DT images are of the size $128 \times 128 \times 48$, with the voxel spacings $1.72 \times 1.72 \times 3.0\,\mathrm{mm}^3$. Each subject is registered to the template first using our affine registration algorithm and followed by the new piecewise affine algorithm. The transformation estimated from the affine registration is used to initialize the following piecewise affine registration.

For visual inspection, the color-coded principal eigenvector maps of one subject after affine registration and after piecewise affine registration are shown together with the template in fig. 2. Notice that the genu, splenium and internal capsules are better aligned after piecewise registration. Moreover, the alignment of the CC after piecewise registration is significantly better than after affine registration.

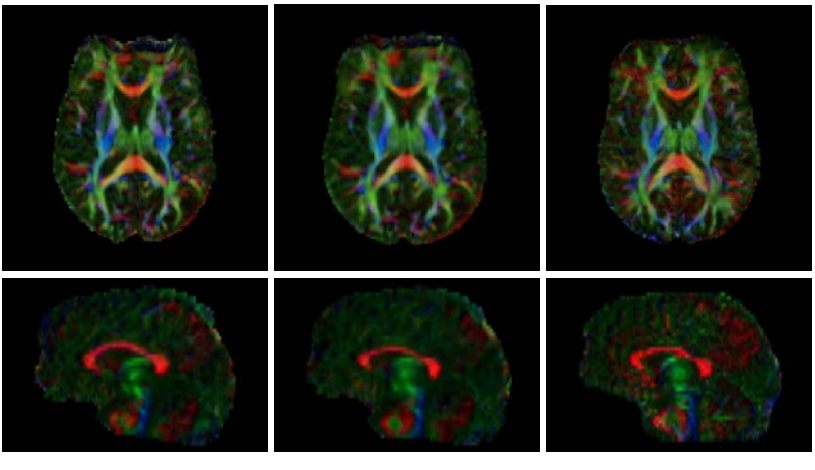

Fig. 2. The color-coded principal eigenvector maps of the axial slice 24 (top row) and the sagittal slice 64 (bottom row) of one of the subjects in this study together with the template. From left to right are the subject after affine registration and after piecewise affine registration, and the template.

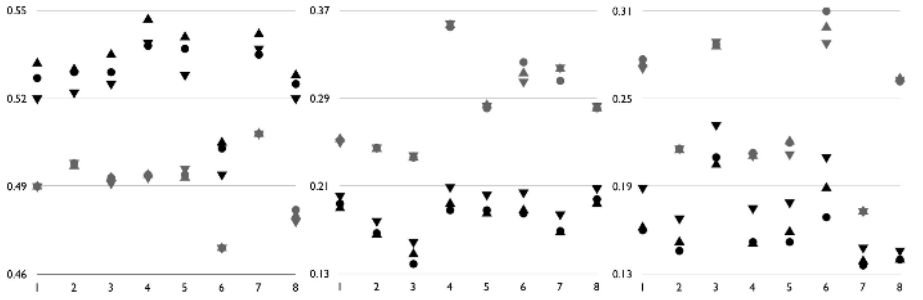

Fig. 3. Quantitative evaluation of registration results: In each graph, the x-axis represents the list of 8 subjects and the y-axis is some evaluated quantity. From left to right, the quantity evaluated are the AOE of all the WM voxels, the AAS of the voxels in the manually segmented CC, and the AAS of the voxels in the manually segmented CST. For each subject, there are six data points in each graph that correspond to six different registration methods, the affine (grey symbols) and piecewise affine (black symbols) registrations with three different DT metrics: TD (inverted triangles), ED (circles) and LD (triangles), and larger AOE or smaller AAS correspond to better alignment.

Quantitative evaluations are done as outlined in section 2.3. The results are summarized in fig. 3. It is evident that, consistent with the observation from visual inspection, the new piecewise algorithm outperforms its affine counterpart consistently for all the metrics tested. The two tensor metrics perform similarly well and they do slightly better than the scalar metric TD.

Finally, the algorithm is computationally efficient. Running on a 3.0GHz Pentium 4 Xeon processor, the computation time of registering each subject is less than 10 minutes.

4 Conclusion

In conclusion, we have presented a piecewise affine algorithm that demonstrates explicit orientation optimization required for optimal matching of DT imagery can be accomodated in deformable registration. Morever, our novel formulation enables fast and accurate optimization using analytic derivatives. Results from inter-subject registration demonstrate the algorithm improves image alignment in a region-specific manner over affine registration. Future work includes more quantitative assessment of the algorithm using larger datasets and analyzing the effect of smoothing of the piecewise affine transformations.

Acknowledgement

This work was supported by the USPHS via NIH grants NS044189, DA015886 and NS045839.

References

1. Basser, P.J., Mattiello, J., Bihan, D.L.: Estimation of the effective self-diffusion tensor from the NMR spin echo. JMR **103** (1994) 247–254
2. Jones, D.K., Simmons, A., Williams, S.C.R., Horsfield, M.A.: Non-invasive assessment of axonal fibre connectivity in the human brain via diffusion tensor MRI. MRM **42** (1999) 37–41
3. Wakana, S., Jiang, H., Nagae-Poetscher, L.M., van Zijl, P.C., Mori, S.: Fiber tract-based atlas of human white matter anatomy. Radiology **230** (2004) 77–87
4. Jones, D.K., Griffin, L.D., Alexander, C.C., Catani, M., Horsfield, M.A., Howard, R., Williams, S.C.R.: Spatial normalization and averaging of diffusion tensor MRI data sets. NeuroImage **17** (2002) 592–617
5. Park, H.J., Kubicki, M., Shenton, M.E., Guimond, A., McCarley, R.W., Maier, S.E., Kikinis, R., Jolesz, F.A., Westin, C.F.: Spatial normalization of diffusion tensor MRI using multiple channels. Med Image Anal **6** (2002) 143–161
6. Alexander, D.C., Pierpaoli, C., Basser, P.J., Gee, J.C.: Spatial transformations of diffusion tensor magnetic resonance images. TMI **20** (2001) 1131–1139
7. Gee, J.C., Alexander, D.C.: Diffusion-tensor image registration. In Welckert, J., Hagen, H., eds.: Visualization and Image Processing of Tensor Fields. Berlin:Springer (2005)
8. Zhang, H., Yushkevich, P., Gee, J.C.: Registration of diffusion tensor images. In: Proc. CVPR. (2004)
9. Hellier, P., Barillot, C., Memin, E., Perez, P.: Hierarchical estimation of a dense deformation field for 3-d robust registration. TMI **20** (2001) 388–402
10. Pajevic, S., Pierpaoli, C.: Color schemes to represent the orientation of anisotropic tissues from diffusion tensor data: application to white matter fiber tract mapping in the human brain. MRM **42** (1999) 526–540
11. Little, J.A., Hill, D.L.G., Hawkes, D.J.: Deformations incorporating rigid structures. Computer Vision and Image Understanding **66** (1997) 223–232
12. Basser, P.J., Pajevic, S.: Statistical artifacts in diffusion tensor MRI (DT-MRI) caused by background noise. MRM **44** (2000) 41–50
13. Curran, K.M., Alexander, D.C.: Orientation coherence optimisation in tensor image registration. In: Proc. MIUA. (2004)